

Limit state condition and the dissipation function for isotropic materials

J. PODGÓRSKI (LUBLIN)

THE PAPER presents the limit state condition containing three stress tensor invariants which may be particularly useful in considering the behaviour of brittle and granular materials. The corresponding power dissipation function is found. This makes it possible to obtain a dual description of the $\sigma - \epsilon$ relation. Particular forms of the dissipation function derived in the paper correspond to the classical limit state conditions and simplify the estimation of the load carrying capacity.

W pracy przedstawiono warunek stanu granicznego zależny od trzech niezmienników tensora naprężenia, szczególnie przydatny do opisu zachowania materiałów kruchych i ośrodków rozdrobnionych. Dla warunku tego znaleziono funkcję dysypacji mocy, co pozwoliło uzyskać dualność opisu zależności $\sigma - \epsilon$. Szczególne postacie funkcji dysypacji odpowiadające klasycznym warunkom stanu granicznego, które podano w pracy, ułatwiają oszacowania nośności granicznej.

В работе представлено условие предельного состояния, зависящее от трех инвариантов тензора напряжения, особенно пригодное для описания поведения хрупких материалов и размельченных сред. Для этого условия найдена функция диссипации мощности, что позволило получить дуальность описания зависимости $\sigma - \epsilon$. Частные виды функции диссипации, отвечающие классическим условиям предельного состояния, которые приведены в работе, облегчают оценки предельной несущей способности.

Nomenclature

- σ stress tensor,
- σ' deviator of the tensor σ ,
- ϵ strain rate tensor,
- ϵ' deviator of the tensor ϵ ,
- $\sigma \cdot \sigma$ denotes $\sigma_{ij} \sigma_{ij}$,
- $\sigma \sigma$ denotes $\sigma_{ik} \sigma_{kj}$,
- I_1, I_2, I_3 invariants of the tensor σ ,
- σ_0 mean normal pressure $\sigma_0 = \frac{1}{3} I_1$,
- J_2, J_3 invariants of the tensor σ' ,
- τ_0 octahedric shearing stress; $\tau_0 = \sqrt{\frac{2}{3} J_2}$,
- φ angle at the deviatoric plane in the space of stresses,
- $J = \cos 3\varphi$ invariant of the tensor σ' ; $J = \frac{3\sqrt{3}}{2} \frac{J_3}{J_2^{3/2}}$,
- II, III invariants of the tensor ϵ' ,

- γ_0 octahedric distortion strain rate, $\gamma_0 = \sqrt{\frac{2}{3} \text{II}}$,
 φ_e angle at the deviatoric plane in the space of strains,
 $J_s = \cos 3\varphi_s$ invariant of the tensor ϵ' ; $J_s = \frac{3\sqrt{3}}{2} \frac{\text{III}}{\text{II}^{3/2}}$,
 $f = 0$ limit state condition,
 ϑ, λ parameters defining the shape of the section of the limit surface by the deviatoric plane,
 $P(J)$ shape function of the limit surface,
 α, β parameters of the shape function $P(J)$,
 C_0, C_1 parameters of the function f ,
 \mathbf{n} normal to the limit surface in the deviatoric plane,
 D power of dissipation,
 μ_1, μ_2 Lagrangean multipliers,
 a arbitrary constant from the interval $\langle 0, 1 \rangle$.

1. Introduction

THE FORMULATION of the limit state criterion for materials, the behaviour of which essentially depends on the third stress tensor invariant and on the mean pressure, is still an open problem.

The commonly used Coulomb–Mohr condition yields the results which differ from the experimental data (for instance in the case of rocks, concrete etc.) by more than ten percent, what is particularly evident in the range of positive mean normal stresses (at the vertex of the limit surface). This is the reason why repeated attempts have been made to determine the limit state more rigorously. Let us mention the papers by LADE and DUNCAN [1], MATSUOKA [2], GUDEHUS [3] in which new criteria for sands are proposed, and also the papers by MILLS, ZIMMERMAN [4], WILLAM and WARNKE [5], OTTOSEN [6] where the failure conditions for concrete are given.

In this paper a condition will be presented which embraces a very important class of conical limit surfaces (a more general condition was formulated by the author in [7]). This criterion contains the classical conditions by Huber–Mises, Tresca, Coulomb–Mohr, Drucker–Prager and also the recently proposed LADE [1] and MATSUOKA [2] conditions; the new criterion enables a more accurate description of the material behaviour. The dissipated power function was also determined for this criterion; this made it possible to represent the relations between the stresses and strain rates in two equivalent, dual forms. Equations for the dissipated power functions correspond to the classical limit state conditions and may be used to solve many practical problems, first of all the upper estimates of the load carrying capacity.

The determination of the dissipated power function in the case of singular limit surfaces (the Tresca and Coulomb–Mohr conditions) and all conical limit surfaces is not an easy task due to nonunique relations between the stress and strain rate tensors. The difficulties were surmounted by means of the limit transformations presented in Sect. 4 and the Lagrange multipliers introduced in Sect. 5.

2. Coordinate systems

In order to simplify the description of the limit surfaces and the dissipated power surfaces, let us apply the cylindrical coordinate systems in the stress and strain rate spaces.

In the space of stresses the cylindrical coordinates (h, r, φ) , Fig. 1, are expressed in terms of the stress tensor by the following formulae:

$$(2.1) \quad \begin{aligned} h &= \frac{\sqrt{3}}{3} I_1 = \sqrt{3} \sigma_0, \\ r &= \sqrt{2J_2} = \sqrt{3} \tau_0, \\ \cos 3\varphi &= J = \frac{3\sqrt{3}}{2} \frac{J_3}{J_2^{3/2}}. \end{aligned}$$

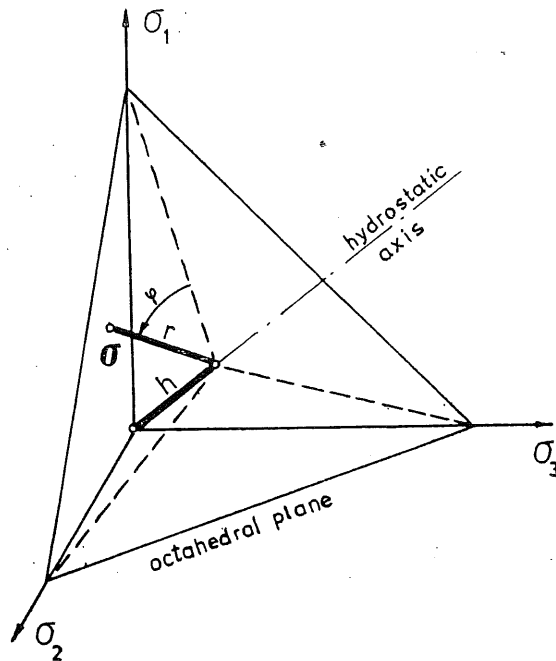


FIG. 1.

Here $I_1 = \text{tr} \boldsymbol{\sigma}$ — first invariant of the stress tensor $\boldsymbol{\sigma}$, $\sigma_0 = \frac{1}{3} I_1$ — mean normal stress, $J_2 = \frac{1}{2} \boldsymbol{\sigma}' \cdot \boldsymbol{\sigma}'$ — second invariant of the stress deviator $\boldsymbol{\sigma}'$, $\tau_0 = \sqrt{\frac{2}{3} J_2}$ — octahedric shearing stress, $J_3 = \frac{1}{3} (\boldsymbol{\sigma}' \boldsymbol{\sigma}') \cdot \boldsymbol{\sigma}'$ — third invariant of the stress deviator $\boldsymbol{\sigma}'$, J — denotes $\cos 3\varphi$.

Analogous relations are assumed for the components h_e, r_e, φ_e in the space of strain and the strain rate tensor invariants,

$$\begin{aligned} h_e &= \frac{\sqrt{3}}{3} \varepsilon_{kk}, \\ r_e &= \sqrt{2\Pi} = \sqrt{3} \gamma_0, \\ \cos 3\varphi_e &= J_e = \frac{3\sqrt{3}}{2} \frac{\text{III}}{\Pi^{3/2}}. \end{aligned}$$

Here ε_{kk} — first invariant of the strain rate tensor ϵ , $\Pi = \frac{1}{2} \epsilon' \cdot \epsilon'$ — the second invariant of the strain rate deviator ϵ' , $\gamma_0 = \sqrt{\frac{2}{3} \Pi}$ — octahedric distortion strain rate velocity, $\text{III} = \frac{1}{3} (\epsilon' \epsilon') \cdot \epsilon'$ — the third invariant of the strain rate deviator ϵ' , J_s — denotes $\cos 3\varphi_s$.

3. Limit state condition

Comparison of the results of experimental investigations with the values predicted by the limit state criteria shows the section of the limit surface made by the deviatoric plane to constitute a very important element of the limit surface. In view of this fact, several authors have proposed different functions to describe the shape of that section. The functions, written in the form $r = r(\varphi)$, or $r = P(J)$, will be called here the shape functions.

The simplest shape functions are

$$r = r_0 - J \quad (\text{MILLS and ZIMMERMAN [4]}),$$

and

$$r^2 = r_0 - J \quad (\text{GUDEHUS [3]}),$$

in which r_0 denotes a constant satisfying the convexity conditions:

$$r_0 \geq 10 \quad \text{for the Mills and Zimmerman functions,}$$

$$r_0 \geq 4 \quad \text{for the Gudehus function.}$$

Owing to these conditions, the ranges of applicability of the criteria are considerably limited since for many materials (e.g. rocks, concrete, sand) it proves to be necessary to apply the section shapes which are almost triangular.

Such a possibility is offered by the shape function proposed by WILLAM and WARNKE [5] who used the equation of an ellipse

$$r = \frac{2(1-\lambda^2)\cos\varphi + (2\lambda-1)\sqrt{4(1-\lambda^2)\cos^2\varphi + 5\lambda^2 - 4\lambda}}{4(1-\lambda^2)\cos^2\varphi + (2\lambda-1)^2},$$

where λ denotes a certain constant equal to the ratio of radii r at $\varphi = 0^\circ$ and $\varphi = 60^\circ$,

$$(3.1) \quad \lambda = \frac{r(0^\circ)}{r(60^\circ)},$$

angle φ varies within the interval $-60^\circ, 60^\circ$.

LADE and DUNCAN [1], MATSUOKA [2] and OTTOSEN [6] use the function given by the formula

$$r = \frac{1}{\cos\left(\frac{1}{3} \arccos \alpha J\right)}$$

with the constant α satisfying the condition $0 \leq \alpha \leq 1$; this function describes the family of curves contained between the circle ($\alpha = 0$) and the triangle ($\alpha = 1$).

Another classical condition of Coulomb–Mohr may be analyzed in this way by introducing the shape function

$$r = \frac{1}{\cos(|\varphi| - \beta)},$$

where β is a constant depending on the angle of internal friction (cf. Table 1), and φ satisfies the condition $0^\circ \leq |\varphi| \leq 60^\circ$.

Table 1.

Criterion	Values of constants			
	C_0	C_1	α	β
HUBER–MISES $J_2 - k^2 = 0$	$\sqrt{\frac{2}{3}} k$	0	0	$\frac{\pi}{6}, P = 1$
TRESCA $ \tau_{\max} - k = 0$	$\sqrt{\frac{2}{3}} k$	0	1	$\frac{\pi}{6}$
DRUCKER–PRAGER $\sqrt{J_2} - a + bI_1 = 0$	$\sqrt{\frac{2}{3}} a$	$\sqrt{6} b$	0	$\frac{\pi}{6}, P = 1$
COULOMB–MOHR $ \tau_n = c - \text{tg } \phi \sigma_n$	$\frac{\sqrt{2} c \cos \phi}{\sqrt{3 + \sin^2 \phi}}$	$\frac{\sqrt{2} \sin \phi}{\sqrt{3 + \sin^2 \phi}}$	1	$\text{arctg} \left(\sqrt{3} \frac{1 - \sin \phi}{3 + \sin \phi} \right)$
LADE, DUNCAN $I_1^3 - \kappa_1 I_3 = 0$	0	$\sqrt{\frac{\kappa_1 - 27}{2\kappa_1}}$	$\sqrt{\frac{\kappa_1 - 27}{2\kappa_1}}$	0
MATSUOKA $\frac{I_1 I_2}{I_3} = 9(K^2 + 1)$	0	$\frac{1}{\sqrt{2 \left(1 + \frac{2}{3K^2} \right)}}$	$\frac{1 + \frac{1}{K^2}}{\sqrt{1 + \frac{2}{3K^2}}}$	0

In order to analyze the possibility of adaptation of these functions to the experimental data, let us introduce, in addition to λ , another characteristic parameter of the cross-section, and namely the ratio of r at $\varphi = 30^\circ$ and at $\varphi = 60^\circ$,

$$(3.2) \quad \vartheta = \frac{r(30^\circ)}{r(60^\circ)}.$$

The ϑ – λ relationships of the shape function and the experimental results concerning concrete, sand and clay are shown in Fig. 2. Comparison of these relationships allows one to draw the conclusion that none of the shape functions used so far enables us to describe the behaviour of brittle and granular materials with sufficient accuracy.

Hence it is necessary to introduce a new function depending on both parameters in order to obtain the ϑ – λ characteristics lying in the entire region bounded from below by the Coulomb–Mohr condition, and from above — by the Lade curve (Fig. 2).

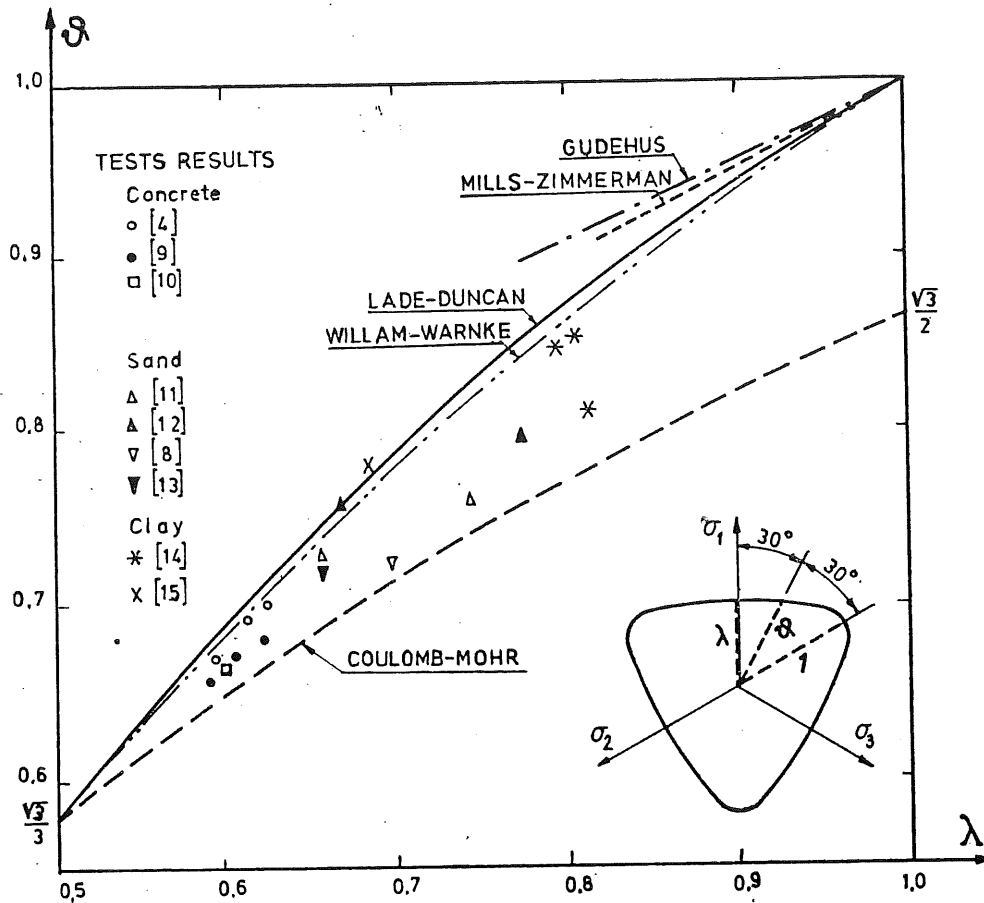


FIG. 2.

The function satisfying the above conditions may be defined by the following equation:

$$(3.3) \quad r = \frac{1}{P(J)}, \quad P(J) = \cos\left(\frac{1}{3} \arccos \alpha J - \beta\right),$$

α , β being the constants satisfying the conditions $0 \leq \alpha \leq 1$, $0^\circ \leq \beta \leq 30^\circ$. The parameters α and β may be determined on the basis of the known characteristics λ , ϑ by means of Eqs. (3.4). The equations are easily solved by the method of consecutive approximations assuming the initial value $\beta = 0^\circ$.

$$(3.4) \quad \begin{aligned} \alpha &= \cos 3x, \\ \operatorname{tg} x &= \frac{\lambda \cos \beta - \cos(60^\circ - \beta)}{\sin(60^\circ - \beta) - \lambda \sin \beta}, \\ \operatorname{tg} \beta &= \frac{2\lambda \cos x - \sqrt{3} \vartheta}{\vartheta - 2\lambda \sin x}. \end{aligned}$$

The shape function in the form (3.3) may be used to construct the general form of the limit state criterion

$$A_0(\sigma_0) + A_1(J) \tau_0 + A_2(J) \tau_0^2 = 0,$$

Here A_0 is a function of the mean pressure σ_0 only, and A_1 , A_2 are functions of J .

This general form of the criterion was used by the author to describe the phenomenon of failure of concrete [7], what leads to a very good agreement with experimental results.

In this paper considerations will be confined to such forms of the limit state condition which lead to the conical limit surfaces:

$$(3.5) \quad f = P(J)\tau_0 - C_0 + C_1\sigma_0 = 0,$$

C_0 and C_1 being constants.

The criterion in the form (3.5) makes it possible to obtain several known limit state conditions by assuming different values of the constants α , β , C_0 and C_1 , what is shown in Table 1.

Let us now discuss the method of determination of the constants α , β , C_0 , C_1 on the basis of the experimental data given by GREEN and BISHOP [8] and concerning packed sand. The results of the investigations taken from Fig. 3 of the paper [8] are presented

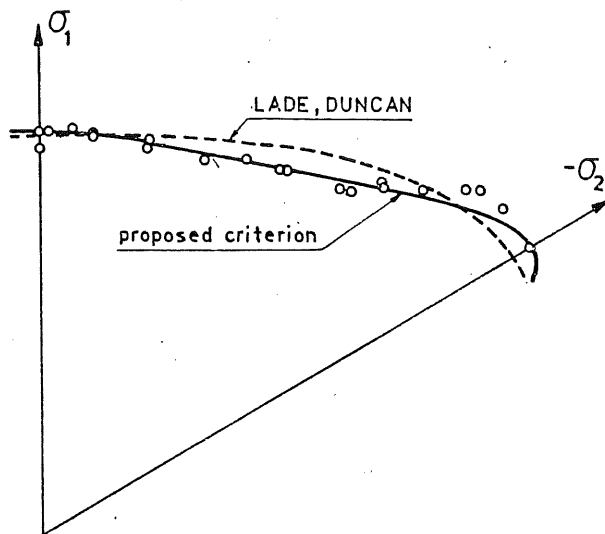


FIG. 3.

in Table 2. Using these results and assuming zero cohesion ($\tau_0 = 0$ for $\sigma_0 = 0$), the characteristics ϑ and λ of the limit surface cross-section are determined from the formulae

$$\lambda = \frac{3/\sin\phi_c - 1}{3/\sin\phi_t + 1},$$

$$\vartheta = \frac{\sin\phi_0}{2\sqrt{3}} (3/\sin\phi_c - 1),$$

Here ϕ_c , ϕ_0 , ϕ_t denote the respective internal friction angles at the three-axial compression ($\varphi = 60^\circ$, $J = -1$), three-axial shear ($\varphi = 30^\circ$, $J = 0$) and three-axial extension ($\varphi = 0^\circ$, $J = 1$).

Table 2.

b	0	0.09	0.14	0.16	0.22	0.27	0.28	0.31	0.33	0.43	0.44	0.51	0.59
φ [deg]	60	55.33	52.57	51.43	47.92	44.87	44.25	42.37	41.11	34.62	33.96	29.34	24.07
ϕ [deg]	39	42.5	44	44	43.5	43.5	44	42	42	43	43	43.5	43

b	0.72	0.86	0.91	0.98	1.0
φ [deg]	15.75	7.43	4.67	1.00	0
ϕ [deg]	45 43.5	45 44	45	44	44 41

$$b = \frac{\sigma_2 - \sigma_3}{\sigma_1 - \sigma_3}, \quad \operatorname{tg} \varphi = \sqrt{3} \left(\frac{1-b}{1+b} \right), \quad \sigma_1 > \sigma_2 > \sigma_3$$

The assumption of zero cohesion makes the constant C_0 in Eq. (3.5) vanish and so, once both parameters α and β are found from the relations (3.4), there remains only one constant C_1 to be determined from the equation

$$C_1 = 2\sqrt{2} \frac{\cos\left(\frac{1}{3}\arccos\alpha - \beta\right)}{3/\sin\phi_t + 1}.$$

From Table 2 we obtain $\phi_t = 44^\circ$, $\phi_c = 39^\circ$ and assume $\phi_0 = 43.5^\circ$ what yields the values $\lambda = 0.7083$, $\vartheta = 0.7486$, $\alpha = 0.9781$, $\beta = 10.28^\circ$, $C_0 = 0$, $C_1 = 0.5291$.

The limit surface section corresponding to these parameters is shown in Fig. 3 (solid line), together with the projections of the experimental points obtained by Green and Bishop [8] and the corresponding curve resulting from the Lade and Duncan condition [1] for $n_1 = 56$ (dashed curve). Comparison of both conditions shows the possibility of a better fitting of the condition proposed to the experimental data.

4. Constitutive relations of a perfectly plastic body

Assuming the associated flow law, the strain rate tensor may be written in the form

$$\epsilon = \dot{\lambda} \frac{\partial f}{\partial \sigma}, \quad \text{where } \dot{\lambda} > 0.$$

This equation may be transformed to another form, more convenient for further considerations:

$$(4.1) \quad \epsilon = \frac{1}{3} \epsilon_{kk} \mathbf{1} + \epsilon', \quad \epsilon' = \dot{\lambda} \mathbf{n},$$

where

$$\mathbf{n} = \frac{\partial f}{\partial \sigma'} = \frac{\partial [P(J)\tau_0]}{\partial \sigma'}.$$

In the case of the condition given by Eq. (3.5), the above relations may be represented in the form

$$(4.2) \quad \epsilon_{kk} = \dot{\lambda} C_1, \\ \mathbf{n} = P \frac{\sigma'}{3\tau_0} + P' \left(\sqrt{2} \frac{\sigma''}{\tau_0^2} - J \frac{\sigma'}{\tau_0} \right),$$

where

$$P' = \frac{\partial P}{\partial J} = \frac{1}{3} \frac{\sin\left(\frac{1}{3}\arccos\alpha J - \beta\right)}{\sqrt{\frac{1}{\alpha^2} - J^2}}, \\ \sigma'' = \frac{\partial J_3}{\partial \sigma'} = \sigma' \sigma' - \tau_0^2 \mathbf{1}.$$

Finally, Eq. (4.1) assumes the form

$$(4.3) \quad \epsilon = \dot{\lambda} \left(\frac{1}{3} C_1 \mathbf{1} + \mathbf{n} \right),$$

which for the different criteria listed in Table 1 remains unchanged ⁽¹⁾, in contrast to the formula determining the deviator \mathbf{n} .

The relation between the deviator \mathbf{n} and the tensor σ for the classical limit state conditions is shown in Table 3.

Table 3.

Criterion	Deviator \mathbf{n}
HUBER-MISES	$\mathbf{n} = \frac{1}{3\tau_0} \sigma'$
TRESCA	$J^2 \neq 1, \quad \mathbf{n} = \overset{(1)}{\mathbf{n}}, \quad \overset{(1)}{n_{ij}} = \frac{1}{\sqrt{2}} \begin{vmatrix} 1 & 0 & 0 \\ 0 & -1 & 0 \\ 0 & 0 & 0 \end{vmatrix}$ $J = 1, \quad \mathbf{n} = a\overset{(1)}{\mathbf{n}} + (1-a)\overset{(2)}{\mathbf{n}}, \quad \overset{(2)}{n_{ij}} = \frac{1}{\sqrt{2}} \begin{vmatrix} 1 & 0 & 0 \\ 0 & 0 & 0 \\ 0 & 0 & -1 \end{vmatrix}$ $J = -1, \quad \mathbf{n} = a\overset{(2)}{\mathbf{n}} + (1-a)\overset{(3)}{\mathbf{n}}, \quad \overset{(3)}{n_{ij}} = \frac{1}{\sqrt{2}} \begin{vmatrix} 0 & 0 & 0 \\ 0 & 1 & 0 \\ 0 & 0 & -1 \end{vmatrix}$
DRUCKER-PRAGER	$\mathbf{n} = \frac{1}{3\tau_0} \sigma'$
COULOMB-MOHR	$J^2 \neq 1, \quad \mathbf{n} = \overset{(2)}{\mathbf{n}}$ $J = 1, \quad \mathbf{n} = a\overset{(1)}{\mathbf{n}} + (1-a)\overset{(2)}{\mathbf{n}} \quad \left(\overset{(1)}{\mathbf{n}}, \overset{(2)}{\mathbf{n}}, \overset{(3)}{\mathbf{n}} \text{ determined by Eqs. (4.6), (4.7), (4.8)} \right)$ $J = -1, \quad \mathbf{n} = a\overset{(2)}{\mathbf{n}} + (1-a)\overset{(3)}{\mathbf{n}}$

Let us now present the method of derivation of that relation in the most complex case of the Coulomb-Mohr criterion. The corresponding limit surface is a pyramid, hence its edges are located at $J^2 = 1$; this accounts for the indefiniteness of the direction of \mathbf{n} in the deviatoric plane. By assuming $J^2 \neq 1$, we may determine the deviator \mathbf{n} for a side of the Coulomb-Mohr pyramid.

⁽¹⁾ This does not apply to the Lade and Matsuoka condition and other conditions in which the constant C_1 appearing in Eq. (3.5) equals zero since the assumption of the associated flow law yields the conclusion of zero dissipation, and this contradicts the experiments. The contradiction may be avoided by assuming the nonassociated flow law. However, this is not the subject of this paper.

Substitution of $\alpha = 1$ in Eq. (4.2)₂ (cf. Table 1) yields

$$(4.4) \quad \mathbf{n} = \frac{\cos \psi}{3\tau_0^2} \left[\tau_0 \boldsymbol{\sigma}' \left(1 - \operatorname{tg} \psi \frac{J}{\sqrt{1-J^2}} \right) + \sqrt{2} \boldsymbol{\sigma}'' \frac{\operatorname{tg} \psi}{\sqrt{1-J^2}} \right],$$

where

$$\psi = \frac{1}{3} \arccos J - \beta = |\varphi| - \beta.$$

From Eq. (4.4) it follows that \mathbf{n} is a normal to a side of the hexagon which represents the section of the Coulomb–Mohr surface made by the deviatoric plane (Fig. 4).

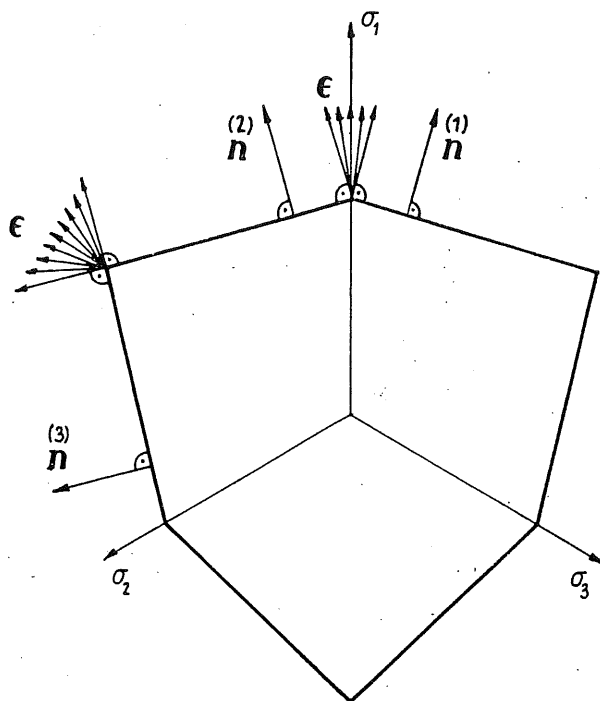


FIG. 4.

In order to verify this property, let us calculate, in accordance with Eq. (2.2)₃, the value of $\cos 3\varphi_s^i = J_s$.

For the deviator \mathbf{n} we obtain

$$(4.5) \quad \begin{aligned} \text{II} &= \frac{1}{2} \dot{\lambda}^2 \mathbf{n} \cdot \mathbf{n} = \frac{\dot{\lambda}^2}{6} [P^2 + 9(P')^2(1-J^2)], \\ \text{III} &= \frac{1}{3} \dot{\lambda}^3 (\mathbf{n} \mathbf{n}) \cdot \mathbf{n} = \frac{\dot{\lambda}^3}{27\sqrt{2}} [P^3 J + 9P^2 P'(1-J^2) \\ &\quad - 27P(P')^2 J(1-J^2) - 27(P')^3(1-J^2)^2]. \end{aligned}$$

On substituting into these equations $\alpha = 1$, $P = \cos \psi$, $P' = 3 \frac{\sin \psi}{3\sqrt{1-J^2}}$ we obtain from Eq. (2.2)₃ $J = \cos 3\beta$ what proves that \mathbf{n} is normal to the side of the hexagon.

Let us now analyze the deviator \mathbf{n} given by Eq. (4.2)₂ at the singular point $J = 1$. In Eq. (4.2)₂ we assume now $P = \cos\beta$, $P' = -\frac{\sin\beta}{3\sqrt{\frac{1}{\alpha^2}-J^2}}$. The following expressions appear in Eqs. (4.5):

$$w_1 = \frac{1-J^2}{\frac{1}{\alpha^2}-J^2} \quad \text{and} \quad w_2 = \frac{1-J^2}{\sqrt{\frac{1}{\alpha^2}-J^2}},$$

their limits at the point $\alpha = 1, J = 1$ being equal to:

$$\lim w_1 = a, \quad \lim w_2 = 0 \quad \text{where} \quad 0 \leq a \leq 1$$

depending on the path at the plane $\alpha - J$ along which the point $(\alpha = 1, J = 1)$ is approached.

Indefiniteness of the limit w_1 is the reason for the indefiniteness of the direction of \mathbf{n} . Equations (4.5) may now be written in the following form:

$$\text{II} = \frac{\lambda^2}{6} (\cos^2\beta + a \sin^2\beta),$$

$$\text{III} = \frac{\lambda^3}{27\sqrt{2}} (\cos^3\beta - 3a \cos\beta \sin^2\beta),$$

$$J = \frac{4}{\varrho^3} \cos^3\beta - \frac{3}{\varrho^2} \cos\beta, \quad \text{where} \quad \varrho = \sqrt{6\text{II}}.$$

By solving this equation for $\sqrt{\text{II}}$ we obtain the equation of a straight line in the octahedric plane

$$\sqrt{\text{II}} = \frac{\cos\beta}{\cos\left(\frac{1}{3} \arccos J_s\right)} = \frac{\cos\beta}{\cos\varphi_s}.$$

The equation remains valid within the interval $|\varphi_s| \leq \beta$, only, what means that the tip of the normal \mathbf{n} moves along a straight line perpendicular to one of the principal directions.

The results obtained make it possible to write the normal \mathbf{n} as a combination of the normals $\mathbf{n}^{(1)}$ and $\mathbf{n}^{(2)}$ of two sides of the Coulomb-Mohr hexagon (cf. Fig. 4):

$$\mathbf{n} = a\mathbf{n}^{(1)} + (1-a)\mathbf{n}^{(2)}, \quad \text{where} \quad 0 \leq a \leq 1.$$

The normals $\mathbf{n}^{(1)}$ and $\mathbf{n}^{(2)}$ are found from Eq. (4.4) by means of the substitutions

$$\mathbf{n} = \mathbf{n}(\psi = \psi_1), \quad \psi_1 = \frac{1}{3} \arccos J - \beta,$$

$$\mathbf{n} = \mathbf{n}(\psi = \psi_2), \quad \psi_2 = \frac{1}{3} \arccos J + \beta$$

or

$$(4.6) \quad \mathbf{n}^{(1)} = \frac{2}{\sqrt{3}} \sum_{i=1}^3 n_i^{(1)} \mathbf{s}_i \otimes \mathbf{s}_i,$$

where \mathbf{s}_i are the unit principal vectors of the tensor $\boldsymbol{\sigma}$, and the principal values $n_i^{(1)}$ are equal to

$$(4.7) \quad \begin{aligned} n_1^{(1)} &= \cos \beta, & n_2^{(1)} &= -\cos(60^\circ - \beta), & n_3^{(1)} &= -\cos(60^\circ + \beta), \\ \mathbf{n}^{(2)} &= \frac{2}{\sqrt{3}} \sum_{i=1}^3 n_i^{(2)} \mathbf{s}_i \otimes \mathbf{s}_i, \end{aligned}$$

$$n_1^{(2)} = \cos \beta, \quad n_2^{(2)} = -\cos(60^\circ + \beta), \quad n_3^{(2)} = -\cos(60^\circ - \beta).$$

At the second vertex of the Coulomb–Mohr hexagon (for $J = -1$) analogous transformations yield

$$\mathbf{n} = a\mathbf{n}^{(2)} + (1-a)\mathbf{n}^{(3)}$$

where $\mathbf{n}^{(3)}$ is normal to a side of the hexagon (Fig. 4),

$$(4.8) \quad \mathbf{n}^{(3)} = \frac{2}{\sqrt{3}} \sum_{i=1}^3 n_i^{(3)} \mathbf{s}_i \otimes \mathbf{s}_i,$$

$$n_1^{(3)} = -\cos(60^\circ + \beta), \quad n_2^{(3)} = \cos \beta, \quad n_3^{(3)} = -\cos(60^\circ - \beta).$$

Finally, the deviator $\boldsymbol{\epsilon}'$ for the Coulomb–Mohr condition may be expressed by the formulae

$$\begin{aligned} \boldsymbol{\epsilon}' &= \dot{\lambda} \mathbf{n}, & \text{where } J^2 &\neq 1, \\ \boldsymbol{\epsilon}' &= \dot{\lambda} [a\mathbf{n}^{(1)} + (1-a)\mathbf{n}^{(2)}], & \text{where } J &= 1, \\ \boldsymbol{\epsilon}' &= \dot{\lambda} [a\mathbf{n}^{(2)} + (1-a)\mathbf{n}^{(3)}], & \text{where } J &= -1, \end{aligned}$$

where $\mathbf{n}^{(1)}, \mathbf{n}^{(2)}, \mathbf{n}^{(3)}$ are given by Eqs. (4.4), (4.6), (4.7) and (4.8).

5. Power of dissipation

The power dissipated in the process of deformation of a perfectly plastic body is determined by the equation

$$D = \boldsymbol{\sigma} \cdot \boldsymbol{\epsilon}.$$

Substitution of the relations (4.1) and (4.2) yields, in view of the condition (3.5), the following result:

$$D = C_0 \dot{\lambda},$$

whence, on eliminating λ by means of Eqs. (4.1)₂ and (4.5)₁ — it follows

$$(5.1) \quad D = 3C_0 \Pi(J_e) \gamma_0.$$

Here $\Pi(J_e)$ is the shape function of the constant dissipation surface section by the deviatoric plane.

The form of the condition (3.5), which is confined to the conical limit surfaces only, makes the constant dissipation surface a plane figure (or a plane curve if $C_1 = 0$) bounded by a certain cone in the space of strain rates.

$$(5.2) \quad w = \varepsilon_{kk} - 3C_1 \Pi(J_e) \gamma_0 = 0.$$

This boundedness results from the fact that the direction normal to a conical surface is constant in the plane containing the vertex of the cone (Fig. 5).

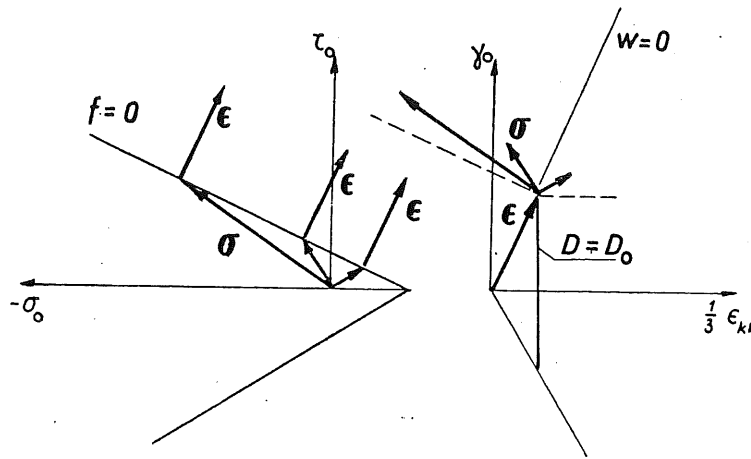


FIG. 5.

The form of the dissipation equation (5.1) and conditions (5.2) is the same for all the limit state criteria shown in Table 1; only the equations determining the shape functions $\Pi(J_e)$ must be different. Equations of the functions $\Pi(J_e)$ corresponding to the classical criteria are given in Table 4.

In order to express the duality of description of the σ - ϵ relation, let us write the stress tensor in the form

$$\sigma = \frac{\partial D}{\partial \epsilon}.$$

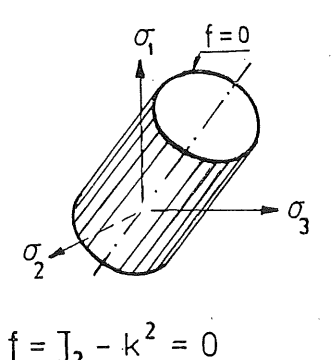
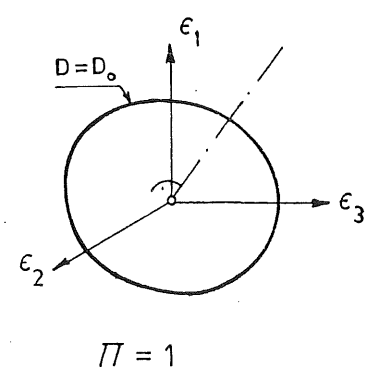
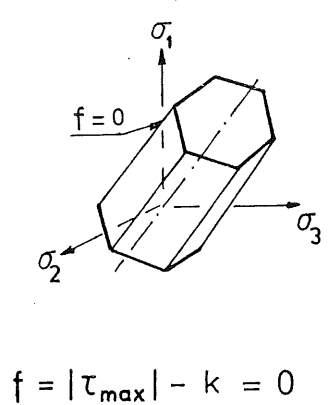
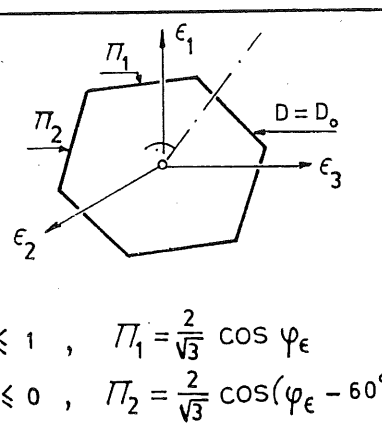
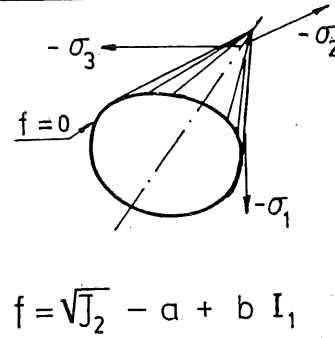
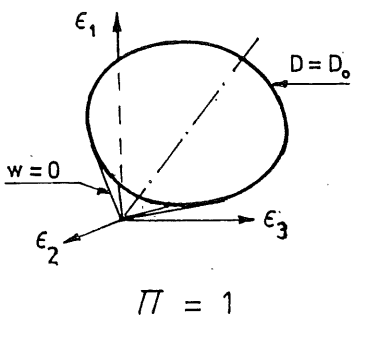
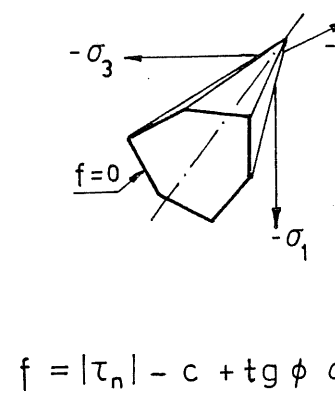
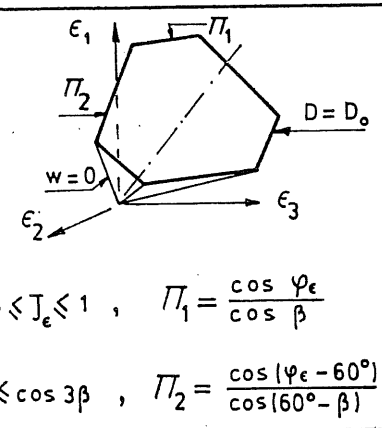
Due to the limitations imposed on the tensor ϵ ($w = 0$, Eq. (5.2)), the relation must be written in a different form.

$$(5.3) \quad \sigma = \frac{\partial D}{\partial \epsilon} + \mu \frac{\partial w}{\partial \epsilon},$$

with μ denoting the Lagrange multiplier.

This equation allows for the determination of the stress deviator only, since in view of the form of the constant dissipation surface the mean pressure σ_0 may be assumed with a certain degree of arbitrariness, ($\sigma_0 \leq C_0/C_1$). It is easily verified that it is the mean press-

Table 4.

$D = 3 C_0 \Pi(J_\epsilon) \gamma_0$, $w = \epsilon_{kk} - 3 C_1 \Pi(J_\epsilon) \gamma_0 = 0$	
Huber-Mises	 <p style="text-align: center;">$f = J_2 - k^2 = 0$</p>  <p style="text-align: center;">$\Pi = 1$</p>
Tresca	 <p style="text-align: center;">$f = \tau_{\max} - k = 0$</p>  <p style="text-align: center;">$\Pi = 1$</p> <p style="text-align: center;"> $0 \leq J_\epsilon \leq 1$, $\Pi_1 = \frac{2}{\sqrt{3}} \cos \varphi_\epsilon$ $-1 \leq J_\epsilon \leq 0$, $\Pi_2 = \frac{2}{\sqrt{3}} \cos(\varphi_\epsilon - 60^\circ)$ </p>
Drucker-Prager	 <p style="text-align: center;">$f = \sqrt{J_2} - a + b I_1$</p>  <p style="text-align: center;">$\Pi = 1$</p>
Coulomb-Mohr	 <p style="text-align: center;">$f = \tau_n - c + \text{tg } \phi \sigma_n$</p>  <p style="text-align: center;">$\Pi = 1$</p> <p style="text-align: center;"> $\cos 3\beta \leq J_\epsilon \leq 1$, $\Pi_1 = \frac{\cos \varphi_\epsilon}{\cos \beta}$ $-1 \leq J_\epsilon \leq \cos 3\beta$, $\Pi_2 = \frac{\cos(\varphi_\epsilon - 60^\circ)}{\cos(60^\circ - \beta)}$ </p>

ure which plays the role of a Lagrange multiplier in Eq. (5.3), and this makes it possible to write the equation in another form:

$$(5.4) \quad \sigma = \sigma_0 \mathbf{1} + 3(C_0 - C_1 \sigma_0) \mathbf{N}.$$

Here $\mathbf{N} = \frac{\partial [II(J_e) \gamma_0]}{\partial \epsilon'}$ is the normal to the curve bounding the constant dissipation surface in the deviatoric plane.

For an arbitrary bounding surface $w = 0$, Eq. (5.2), the tensor \mathbf{N} is expressed by the formula

$$(5.5) \quad \mathbf{N} = \pi \frac{\epsilon'}{\gamma_0} + 3II' \left(\sqrt{2} \frac{\epsilon''}{\gamma_0^2} - J_e \frac{\epsilon'}{\gamma_0} \right),$$

where $II' = \frac{\partial II}{\partial J_e}$, and $\epsilon'' = \epsilon' \epsilon' - \gamma_0 \mathbf{1}$, like the normal \mathbf{n} (cf. Eq. (4.2)). In Table 5 the equations are also given, determining the normal \mathbf{N} for all the classical limit states criteria.

Let us now determine the deviator \mathbf{N} in the case of the Coulomb-Mohr criterion.

Table 5.

$\sigma = \sigma_0 \mathbf{1} + 3(C_0 - C_1 \sigma_0) \mathbf{N}$	
Criterion	Deviator \mathbf{N}
HUBER-MISES	$\mathbf{N} = \frac{1}{3\gamma_0} \epsilon'$
TRESCA	$0 < J_e \leq 1, \quad \mathbf{N} = \overset{(1)}{\mathbf{N}}, \quad \overset{(1)}{N}_{ij} = \sqrt{\frac{2}{3}} \begin{vmatrix} 2 & 0 & 0 \\ 0 & -1 & 0 \\ 0 & 0 & -1 \end{vmatrix}$ $-1 \leq J_e < 0, \quad \mathbf{N} = \overset{(2)}{\mathbf{N}}, \quad \overset{(2)}{N}_{ij} = \sqrt{\frac{2}{3}} \begin{vmatrix} 1 & 0 & 0 \\ 0 & 1 & 0 \\ 0 & 0 & -2 \end{vmatrix}$ $J_e^n = 0, \quad \mathbf{N} = a \overset{(1)}{\mathbf{N}} + (1-a) \overset{(2)}{\mathbf{N}}$
DRUCKER-PRAGER	$\mathbf{N} = \frac{1}{3\gamma_0} \epsilon'$
COULOMB-MOHR	$\cos 3\beta < J_e \leq 1, \quad \mathbf{N} = \overset{(1)}{\mathbf{N}}, \quad \overset{(1)}{N}_{ij} = \frac{1}{\sqrt{2} \cos \beta} \begin{vmatrix} 2 & 0 & 0 \\ 0 & -1 & 0 \\ 0 & 0 & -1 \end{vmatrix}$ $-1 \leq J_e < \cos 3\beta, \quad \mathbf{N} = \overset{(2)}{\mathbf{N}}, \quad \overset{(2)}{N}_{ij} = \frac{1}{\sqrt{2} \cos \left(\frac{\pi}{3} - \beta \right)} \begin{vmatrix} 1 & 0 & 0 \\ 0 & 1 & 0 \\ 0 & 0 & -2 \end{vmatrix}$ $J_e^n = \cos 3\beta, \quad \mathbf{N} = a \overset{(1)}{\mathbf{N}} + (1-a) \overset{(2)}{\mathbf{N}}$

The shape function of the constant dissipation surface is in this case given by the equations (cf. Table 4)

$$\Pi(J_s) = \Pi_1 = \frac{\cos \varphi_s}{\cos \beta} \quad \text{for} \quad \cos 3\beta \leq J_s \leq 1$$

and

$$\Pi(J_s) = \Pi_2 = \frac{\cos(\varphi_s - 60^\circ)}{\cos(60^\circ - \beta)} \quad \text{for} \quad (-1) \leq J_s \leq \cos 3\beta.$$

The analogy of the formulae (5.5) and (4.2)₂ may be used to write, on the basis of Eq. (4.5), the equations

$$(5.6) \quad \begin{aligned} \mathbf{N} \cdot \mathbf{N} &= 3 [\Pi^2 + 9(\Pi')^2(1 - J_s^2)], \\ (\mathbf{NN}) \cdot \mathbf{N} &= \frac{3}{\sqrt{2}} [\Pi^3 J_s + 9\Pi^2(\Pi')(1 - J_s) - 27\Pi(\Pi')^2 J_s(1 - J_s^2) - 27(\Pi')^3(1 - J_s^2)^2], \end{aligned}$$

and

$$J = \frac{3}{2\sqrt{2}} \frac{(\mathbf{NN}) \cdot \mathbf{N}}{(\mathbf{N} \cdot \mathbf{N})^{3/2}}.$$

Substituting here $\Pi = \Pi_1$ and $\Pi = \Pi_2$ we obtain

$$\mathbf{N}^{(1)} = \frac{\partial(\Pi_1 \gamma_0)}{\partial \boldsymbol{\epsilon}'}, \quad \mathbf{N}^{(1)} \cdot \mathbf{N}^{(1)} = \frac{3}{\cos^2 \beta}, \quad J(\mathbf{N}^{(1)}) = 1,$$

and

$$\mathbf{N}^{(2)} = \frac{\partial(\Pi_2 \gamma_0)}{\partial \boldsymbol{\epsilon}'}, \quad \mathbf{N}^{(2)} \cdot \mathbf{N}^{(2)} = \frac{3}{\cos^2(60^\circ - \beta)}, \quad J(\mathbf{N}^{(2)}) = -1,$$

what demonstrates that $\mathbf{N}^{(1)}$ and $\mathbf{N}^{(2)}$ are normal to the hexagon of constant dissipation, Fig. 6.

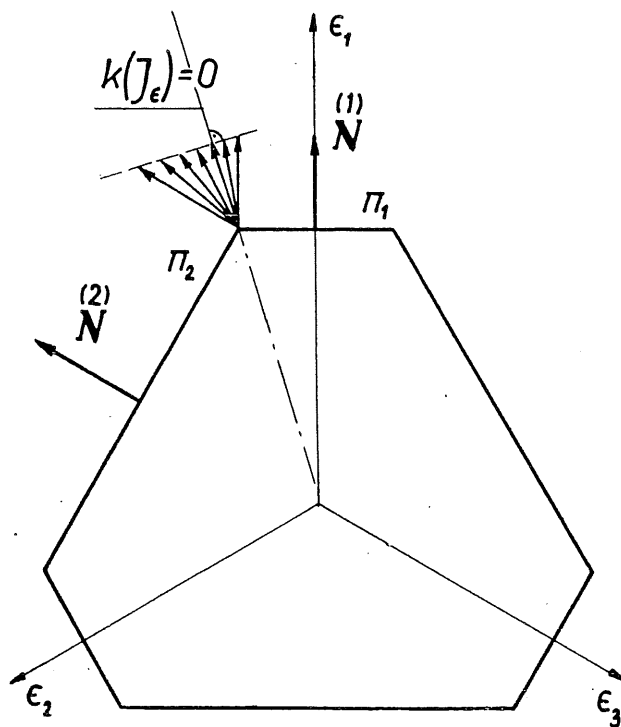


FIG. 6.

The normals $\overset{(1)}{\mathbf{N}}$ and $\overset{(2)}{\mathbf{N}}$ may also be written by means of the following formulae:

$$(5.7) \quad \overset{(1)}{\mathbf{N}} = \frac{\sqrt{2}}{\cos\beta} \sum_{i=1}^3 \overset{(1)}{N}_i \mathbf{e}_i \otimes \mathbf{e}_i,$$

where \mathbf{e}_i are the unit principal vectors of the tensor $\boldsymbol{\epsilon}$, and $\overset{(1)}{N}_1 = 1$, $\overset{(1)}{N}_2 = -1/2$, $\overset{(1)}{N}_3 = -1/2$,

$$(5.8) \quad \overset{(2)}{\mathbf{N}} = \frac{\sqrt{2}}{\cos(60^\circ - \beta)} \sum_{i=1}^3 \overset{(2)}{N}_i \mathbf{e}_i \otimes \mathbf{e}_i,$$

$$\overset{(2)}{N}_1 = \frac{1}{2}, \quad \overset{(2)}{N}_2 = \frac{1}{2}, \quad \overset{(2)}{N}_3 = -1.$$

A separate treatment is needed to determine the deviator \mathbf{N} at the point of intersection of the surfaces Π_1 and Π_2 , that is at the vertex of the constant dissipation cone. Here the five components of the deviator $\boldsymbol{\epsilon}'$ must satisfy the additional condition $J_s = \cos 3\beta$.

This condition may be treated as a constraint imposed on the tensor $\boldsymbol{\epsilon}'$, and so the condition (5.4)₂ is rewritten as

$$(5.9) \quad \mathbf{N} = \frac{\partial(\Pi_1 \gamma_0)}{\partial \boldsymbol{\epsilon}'} - \mu_1 \frac{\partial k(J_s)}{\partial \boldsymbol{\epsilon}'},$$

$$\mathbf{N} = \frac{\partial(\Pi_2 \gamma_0)}{\partial \boldsymbol{\epsilon}'} + \mu_2 \frac{\partial k(J_s)}{\partial \boldsymbol{\epsilon}'}$$

Here $k(J_s) = J_s - \cos 3\beta = 0$ is the equation of constraints, and μ_1 and μ_2 are the Lagrange multipliers. The „-“ sign in the first equation results from the direction of the normal to the plane $k(J_s) = 0$ (Fig. 6).

Denoting $\partial k / \partial \boldsymbol{\epsilon}' = \mathbf{M}$, Eqs. (5.9) are written in a form more convenient for further considerations,

$$(5.10) \quad \text{or} \quad \mathbf{N} = \overset{(1)}{\mathbf{N}} - \mu_1 \mathbf{M},$$

$$\mathbf{N} = \overset{(2)}{\mathbf{N}} + \mu_2 \mathbf{M} \quad \text{from} \quad \mathbf{M} = \frac{1}{\mu_1 + \mu_2} (\overset{(1)}{\mathbf{N}} - \overset{(2)}{\mathbf{N}}).$$

This equation is easily verified to be true in view of the equality

$$\frac{\partial}{\partial \boldsymbol{\epsilon}'} [\gamma_0 (\Pi_1 - \Pi_2)] = (\mu_1 + \mu_2) \frac{\partial k}{\partial \boldsymbol{\epsilon}'},$$

which results from the fact that $k(J_s) = 0$ is the solution of the set of equations

$$D_0 = 3C_0 \Pi_1(J_s) \gamma_0,$$

$$D_0 = 3C_0 \Pi_2(J_s) \gamma_0,$$

valid for arbitrary D_0 . These equations express the condition of equal dissipation at both segments of the curve and at the vertex of the constant dissipation curve.

Equations (5.10) may be written in the form

$$\mathbf{N} = \frac{1}{2} [\mathbf{N}^{(1)} + \mathbf{N}^{(2)} + (\mu_2 - \mu_1)\mathbf{M}],$$

or

$$\mathbf{N} = a\mathbf{N}^{(1)} + (1-a)\mathbf{N}^{(2)}, \quad \text{where} \quad a = \frac{\mu_2}{\mu_1 + \mu_2},$$

$$0 \leq a \leq 1.$$

Consequently, the stress tensor in the case of the Coulomb–Mohr condition is expressed by the formula

$$\boldsymbol{\sigma} = \sigma_0 \mathbf{1} + 3(C_0 - C_1 \sigma_0)\mathbf{N},$$

where

$$\mathbf{N} = \begin{cases} \mathbf{N}^{(1)}, & \text{when } \cos 3\beta \leq J_s \leq 1, \\ \mathbf{N}^{(2)}, & \text{when } -1 \leq J_s \leq \cos 3\beta, \\ a\mathbf{N}^{(1)} + (1-a)\mathbf{N}^{(2)}, & \text{when } J_s = \cos 3\beta, \end{cases}$$

deviators $\mathbf{N}^{(1)}$ and $\mathbf{N}^{(2)}$ being determined by Eqs. (5.7) and (5.8).

6. Conclusions

In the present paper the limit state condition for isotropic materials has been derived; the condition is applicable to a very important (from the practical point of view) class of conical limit conditions.

This criterion contains the classical limit state conditions introduced by Huber–Mises, Tresca, Coulomb–Mohr, Drucker–Prager, and also the recently proposed LADE [1] and MATSUOKA [2] conditions; it enables a more accurate description of the material behaviour, as it was illustrated by the example.

The analytic form of the criterion enabled a simple derivation of the function of power dissipation associated with the limit state conditions which correspond to both the smooth and the singular limit surfaces. The function used as the stress tensor potential allows for the dual description of the $\boldsymbol{\sigma}$ – $\boldsymbol{\epsilon}$ relation.

The dissipation potentials given in the paper may be applied to all classical criteria; this should simplify the procedure of solving numerous practically important problems of the load carrying capacity and, in particular, the evaluation of the upper estimates by means by the kinematically admissible velocity fields.

Within the class of the conditions considered, the strain rate tensor components are not independent. The existence of certain relations holding between the individual components (due to the singular limit surfaces) was treated in the paper as the additional set of constraints imposed on the tensor $\boldsymbol{\epsilon}$; this, in turn, made it possible to apply (after formulation of the constraint equations) the Lagrange multipliers technique.

Acknowledgement

The paper was prepared during the authors stay at the Institute of Fundamental Technological Research, Polish Academy of Sciences, in Warsaw. The author wants to express his gratitude to Professor Z. MRÓZ for the inspiration, and to Assistant Professor B. RANIECKI for valuable, remarks and help in preparing the paper.

References

1. P. V. LADE, J. M. DUNCAN, *Elastoplastic stress-strain theory for cohesionless soil*, J. Geotech. Eng. Div., ASCE, **101**, GT10, Proc. Paper 11670, 1037-1053, Oct. 1975.
2. H. MATSUOKA, *On the significance on the spatial mobilized plane*, Soil and Found., **16**, 1, Jap. Soc. Soil. Mech. Found. Eng., March 1976.
3. G. GUDEHUS, *Elastoplastische Stoffgleichungen für trockenen Sand*, Ing. Archiv., **42**, 3, 1973.
4. L. L. MILLS, R. M. ZIMMERMAN, *Compressive strength of plain concrete under multiaxial loading conditions*, Journ. ACI., **10**, Proc. V67, October 1970.
5. K. J. WILLAM, E. P. WARNKE, *Constitutive model for the triaxial behaviour of concrete*, Int. Ass. Bridge Str. Eng. Colloquium Concrete Structures Subjected to Triaxial Stresses, p. III 1, Bergamo 1974.
6. N. S. OTTOSEN, *A failure criterion for concrete*, J. Eng. Mech. Div., ASCE, **103**, EM4, Proc. Paper 13111, 527-535, August 1977.
7. J. PODGÓRSKI, *General limit state condition for isotropic materials*, IFTR Reports, 17/1983, [in Polish].
8. G. E. GREEN, A. W. BISHOP, *A note on the drained strength of sand under generalized strain conditions*, Geotechnique, **19**, 1, 144-149, London 1969.
9. H. KUPFER, *Das Verhalten des Betons unter mehrachsiger Kurzzeitbelastung unter besonderer Berücksichtigung der zweiachsigen Beanspruchung*, Deutscher Ausschuss für Stahlbeton, H. 229, Berlin 1973.
10. E. TASUJI, F. O. SLATE, A. H. NILSON, *Stress-strain response and fracture of concrete in biaxial loading*, J. ACI, **7**, Proc. V75, July 1978.
11. P. V. LADE, J. M. DUNCAN, *Cubical triaxial tests on cohesionless soil*, J. Soil Mech. Found. Div., ASCE, **99**, SM10, October 1973.
12. H. Y. KO, R. F. SCOTT, *Deformation of sand at failure*, J. Soil Mech. Found. Div., ASCE, **94**, SM4, July 1968.
13. D. C. PROCTER, L. BARDEN, *Correspondence on Green and Bishop: A note on the drained strength of sand under generalized strain conditions*, Geotechnique, **19**, 3, 1969.
14. P. V. LADE, H. MUSANTE, *Three-dimensional behaviour of remolded clay*, J. Geotech. Eng. Div., ASCE, **104**, GT2, February 1978.
15. T. SHIBATA, D. KARUBE, *Influence of the variation of the intermediate principal stress and mechanical properties of normally consolidated clays*, Proc. 6-th Int. Conf. Soil Mech. Found. Eng., Montreal 1965.

TECHNICAL UNIVERSITY OF LUBLIN.

Received October 5, 1983.